'88 KACC 1988. 10. 21~22

# Decoupled Control of Induction Motors for both High Power Efficiency and High Dynamic Performance

°Dong-Il Kim, Myoung-Sam Ko, In-Joong Ha, and Jae-Wha Park

Deptpartment of Control and Instrumentation Engineering
Seoul National University

**Abstract:** In induction motor control, power efficiency as well as high dynamic performance is important. We attempt to achieve both of them by decoupled control of rotor speed and flux. A nonlinear feedback controller with a well-known rotor flux observer is proposed with its stability analysis. Experimental results demonstrate that the proposed control method based on recently developed nonlinear feedback control theory is of practical use.

## 1. Introduction

The recent rapid growth in microprocessor technologies facilitates application of computationally complex control methods to be applied in many industrial problems. Since the so called vector control pioneered by Blaschke [1], there have been a number of notable researches toward high dynamic performance of induction motors [2]-[5]. The underlying idea of their control methods is to make the induction motor behave like a DC motor by controlling the rotor flux constant. A good survey on induction motor control is found in [6].

Except for speed response, there are other important factors to be considered in the controller design of induction motors. Among them is power efficiency. High power efficiency can be obtained by minimizing iron losses and copper losses. It is known that given a constant rotor speed there is an optimal slip speed which leads to maximal power efficiency. Various control methods for high power efficiency can be found in [7]-[11].

Along with remarkable advances in differential geometric control theory [12]-[16], its recent results have been successfully applied to induction motors [17], [18]. In this approach, the nonlinear dynamic equations of the induction motor are transformed into a linear system via appropriate nonlinear feedback. Then, well-known results in linear control theory are employed.

In this paper, we attempt to achieve high power efficiency as well as high dynamic performance by means of decoupled control of rotor speed and flux proposed in [19]. Recently developed nonlinear feedback control theories are utilized. The approach in [19] differs from the prior works in the following aspects. While the prior results are promising and have their own merits, full state feedback is required [17], [18] or full linearization is not obtained [3]-[5]. In practice, rotor fluxes can be measured directly through flux-coils or Hall-probes [1], [20]. However, it is more cost-effective to estimate rotor fluxes based on the rotor circuit equations [6], [21], [22], [23], [24]. Motivated by the prior results, we construct a nonlinear feedback controller with a well-known rotor flux observer in vector control [6], [21], [22]. After sufficient time of motor operation, the speed dynamic characteristics of the induction motor with our controller become linear, while the slip speed is automatically adjusted to be optimal for maximal power efficiency. Thereby, we achieve high power efficiency as well as high dynamic performance. This is made possible by decoupled control of rotor speed and flux proposed in [19].

We provide the stability analysis of the closed-loop system with our controller. Both simulation and experimental results are included to demonstrate the practical significance of our result. In particular, our experimental results contribute to showing that the proposed conroller based on recently developed nonlinear feedback control techniques is of practical use.

## 2. Main Result

The dynamic equations of an induction motor with p pole pairs can be written in the d-q coordinate system rotating synchronously with an angular speed $w_s$ as

$$\begin{aligned}
\dot{i}_{ds} &= -a_1 i_{ds} + \omega_s i_{qs} + a_2 \phi_{dr} + p a_3 \omega_r \phi_{qr} + c V_{ds} \\
\dot{i}_{qs} &= -\omega_s i_{ds} - a_1 i_{qs} - p a_3 \omega_r \phi_{dr} + a_2 \phi_{qr} + c V_{qs} \\
\dot{\phi}_{dr} &= -a_4 \phi_{dr} + a_5 i_{ds} + (\omega_s - p\omega_r)\phi_{qr} \\
\dot{\phi}_{qr} &= -a_4 \phi_{qr} + a_5 i_{qs} - (w_s - p\omega_r)\phi_{dr} \qquad (2.1)
\end{aligned}$$

$$\dot{\omega}_r = \frac{(-B\omega_r + T_e - T_L)}{J}, \qquad (2.2)$$

where $T_e$ is the generated torque given by

$$T_e = K_T(\phi_{dr} i_{qs} - \phi_{qr} i_{ds}). \qquad (2.3)$$

Here, $V_{ds}$, $V_{qs}$, $\omega_s$ are the control inputs available to controller designers and $a_i$, i=1,..,5 are the parameters of the induction motor. Definitions of the symbols used frequently in the developments are given in Nomenclature.

First, we describe our controller for high power efficiency as well as high dynamic performance in induction motors characterized by the above (2.1)-(2.3). Our controller can provide a fast/accurate dynamic response to the rotor speed command and regulate the slip speed at

the optimum value for the maximal efficiency. The controller has the form:

$$u = \begin{bmatrix} V_{ds} \\ V_{qs} \end{bmatrix} = \begin{bmatrix} -\dfrac{\omega_s i_{qs}}{c} + \hat{u}_1 \\ \dfrac{p\omega_r(i_{ds}+a_3\hat{\phi}_{dr})}{c} + \dfrac{\hat{u}_2}{\hat{\phi}_{dr}} \end{bmatrix}, \tag{2.4}$$

where $\hat{\phi}_{dr}$ is obtained by the observer [6], [21], [22]:

$$\dot{\hat{\phi}}_{dr} = -a_4\hat{\phi}_{dr} + a_5 i_{ds}, \tag{2.5}$$

and

$$\omega_s = p\omega_r + a_5\frac{i_{qs}}{\hat{\phi}_{dr}}. \tag{2.6}$$

The new inputs $\hat{u}_1$, $\hat{u}_2$ are given by the IP (Integral-proportional) controllers. IP controllers [25] can provide better transient dynamic responses than the usual PI controllers.

$$\hat{u}_1 = -K_{c\phi} i_{ds} - K_{p\phi}\hat{\phi}_{dr} + K_{i\phi}\int_0^t (k^*|\hat{u}_2|^{\frac{1}{2}} - \hat{\phi}_{dr})\,dt, \tag{2.7}$$

$$\hat{u}_2 = -K_{c\omega}\hat{\phi}_{dr} i_{qs} - K_{p\omega}\omega_r + K_{i\omega}\int_0^t (\omega_r^* - \omega_r)\,dt.$$

and $K_{i\phi}$, $K_{p\phi}$, $K_{c\phi}$, $K_{i\omega}$, $K_{p\omega}$, and $K_{c\omega}$ are the controller gains. Here, $\omega_r^*$ is the rotor speed command, $\omega_{sl}^*$ is the optimal slip speed for maximal power efficiency when $\omega r=\omega_r^*$, and

$$k^* = \left[\frac{ca_5}{(a_1+a_4+cK_{c\omega})\omega_{sl}^*}\right]^{\frac{1}{2}} \tag{2.8}$$

If $\hat{\phi}_{dr}=\phi_{dr}$ and $\phi_{qr}=0$, the controller (2.4), (2.6) linearly decouples the system (2.1)-(2.3) with the output defined $\vec{y}=[\phi_{dr}\ \ \omega_r]$. The IP controllers in (2.7) with (2.8) are to confirm $\omega_r \to \omega_r^*$ and $\omega_{sl} \to \omega_{sl}^*$ in the steady state when $\omega_r^*$ and $T_L$ are constant.

Before stating our theorem, some discussions would be helpful for readers to catch up the main idea of our approach. Let $x \triangleq [x_1 \cdots x_8]^T$ where $x_1 \triangleq i_{ds}$, $x_2 \triangleq \phi_{dr}$, $x_3 \triangleq \int (k^*|\hat{u}_2| - \phi_{dr})dt$, $x_4 \triangleq i_{qs}$, $x_5 \triangleq \omega_r$, $x_6 \triangleq \int(\omega_r^* - \omega_r)dt$, $x_7 \triangleq \phi_{qr}$, and $x_8 \triangleq \hat{\phi}_{dr}$. Let $y \triangleq \omega_r$. Then, the closed-loop system given by (2.1)-(2.8) can be written as

$$\dot{x} = F(x,\omega_r^*) + G(x)\omega_r^* + HT_L,\quad y = x_5, \tag{2.9}$$

where the detailed structures of F, G, and H are given in Appendix A. The dynamic behavior of the system (2.9) is hard to be analyzed in its present form. For this reason, the following state transformation is introduced. Let $w \triangleq [z\ \ e]^T$, $z \triangleq [z_1 \cdots z_6]^T$ and $e \triangleq [e_1\ \ e_2]^T$. In the new coordinate system of state variables defined by

$$w \triangleq T(x) = [x_1\ \ x_2\ \ x_3\ \ (x_2x_4)\ \ x_5\ \ x_6\ \ x_7\ \ (x_2-x_8)]^T, \tag{2.10}$$

the system (2.9) is represented as

$$\dot{w} = \begin{bmatrix} \dot{z} \\ \dot{e} \end{bmatrix} = \begin{bmatrix} Az + (f(w)+g_1(w,\omega_r^*))e + g_2(z,\omega_r^*) + B\omega_r^* + \hat{H}T_L \\ h(w)e \end{bmatrix}$$

$$y = z_5, \tag{2.11}$$

where the detailed structures of f, h, $g_1$, $g_2$, A, B, and $\hat{H}$ are given in Appendix A. Note that the input-output dynamic characteristics of (2.11) are the same as those of (2.9) since only the state transformation (2.10) is involved between two systems (2.9) and (2.11).

Now, we discuss the special case of e=0 in (2.11). The system (2.11) is then reduced to the "almost" linear system:

$$\dot{z}_m = Az_m + g_2(z_m,\omega_r^*) + B\omega_r^* + \hat{H}T_L,$$
$$y_m = (z_m)_5. \tag{2.12}$$

The block diagram representation of (2.12) is shown in Fig.2.1. Observe that the system (2.12) consists of a series connection of two independent linear subsystems. The output response $y_m$ to the command input $\omega_r^*$ is completely determined by the lower subsystem. Hence, any abrupt change in $\omega_{sl}^*$ will not affect the rotor speed response.

It is shown in [7]-[9], [11] that, in the steady state, (i) there is an optimal slip angular speed $\omega_{sl}^*$ for maximum power efficiency and (ii) the optimal slip angular speed is a funtion (say f) of $\omega_r$ (that is, $\omega_{sl}^* = f(\omega_r)$). In particular, such an optimal slip function $f(\omega_r)$ is obtained exeperimentally rather than analytically. Various control methods to make $\omega_{sl}=f(\omega_r)$ at steady state are found in [7]-[9], [11].

In the next Theorem, we show that the dynamic behavior of the closed-loop system (2.1)-(2.8) eventually approaches that of the ideal system (2.12).

Theorem 2.1 Suppose that

(A.1) A is a stable matrix.
(A.2) For each $\omega_r^*:[0,\infty)\to\Omega_2$, $T_L:[0,\infty)\to\Omega_T$, and $x(0)\in\Omega_x$, the system (2.1)-(2.8) has a uni unique solution $x:[0,\infty)\to\Omega_x$.

Then, the controller given by (2.4)-(2.8) assures that

$$|y-y_m| \to 0 \text{ and } \phi_{qr} \to 0 \text{ as } t\to\infty \tag{2.13}$$

where y, $y_m$ are the outputs of the systems (2.11), (2.12), respectively. Furthermore, when $\omega_r^*$ and $T_L$ are constant,

$$\omega_r \to \omega_r^* \text{ and } \omega_{s1} \to \omega_{s1}^* \text{ as } t \to \infty \qquad (2.14)$$

Proof

Let w, $z_m$ denote the states of the systems (2.11), (2.12), respectively. By the arguments similar to those used in [19], it can be shown that

$$\| [(z_4-(z_m)_4)\ (z_5-(z_m)_5)\ (z_6-(z_m)_6)]^T \|$$
$$\text{and} \quad |e| \to 0 \text{ as } t \to \infty \qquad (2.15)$$

This imples (2.13). Next, suppose that $\omega_r^*$ and $T_L$ constant. The block diagram representation of the system (2.12) is shown in Fig.2.1. From Fig.2.1, we can easily see that

$$\hat{u}_2 \to \frac{(a_1+a_4+cK_{c\omega})(B\omega_r^*+T_L)}{cK_T}, \quad y_m \to \omega_r^*,$$
$$\text{and } (z_m)_4 \to \frac{(B\omega_r^*+T_L)}{K_T} \text{ as } t \to \infty. \qquad (2.16)$$

By (2.7), (2.8), (2.15), and (2.16),

$$\omega_r \to \omega_r^*, \quad |\phi_{dr}^*|^2 \to \frac{a_5(B\omega_r^*+T_L)}{K_T\omega_{s1}^*},$$
$$\text{and } z_4 \to \frac{(B\omega_r^*+T_L)}{K_T} \text{ as } t \to \infty. \qquad (2.17)$$

On the other hand, by (2.6) and (2.13),

$$\omega_{s1} = a_5 \frac{z_4}{|\phi_{dr}|^2} \qquad \text{at the steady state} \qquad (2.18)$$

Then, (2.14) follows from (2.16), (2.17) and the Theorem in [19].

From Theorem 2.1, we see that the rotor speed response of the closed-loop system (2.1)-(2.8) follows closely that of the lower linear subsystem of the system in Fig.2.1. Regardless of any constant load torque, the rotor speed and slip speed are regulated at their desired values $\omega_r^*$ and $\omega_{sl}^*$, respectively, in the steady state. Hence our controller (2.4)-(2.8) can drive the induction motor (2.1)-(2.3) with high dynamic performance and high power efficiency. Note that the system in Fig.2.1 is basically the one obtained by a series connection of two independent subsystems in [19]. In fact, the system in Fig.2.1 provides the same linear dynamic chracteristics of the rotor speed as the system in [19].

We need some comments on the assumptions (A.1) and (A.2). From Fig.2.1, we see that (A.1) can be always satisfied by appropriate choice of the controller gains, $K_{i\phi}$, $K_{p\phi}$, $K_{c\phi}$, $K_{i\omega}$, $K_{p\omega}$, and $K_{c\omega}$. The assumption (A.2) is needed for simplicity of proof. It can be removed by imposing restrictions on the allowable sizes of $\Omega_1 \times \Omega_2$, $\Omega_T$, and $|x(0)|$. Then, the proof of Theorem 2.1 becomes more complicated. Moreover, (2.13) and (2.14) hold locally rather than globally.

Finally, we discuss at some length the prior result related to our controller in the following remarks.

Remark 2.1 In [10], the optimal slip function $f(\omega_r)$ need not be predetermined. Instead, a watt-meter is used to determine the input power. Then, the rotor flux is continuously adjusted until maximal power efficiency is reached. However, such changes in the rotor flux result in undesirable disturbances in the rotor speed response. This drawback can be removed by incoorperating our decoupled control approach into his adaptive efficiency controller for the rotor flux.

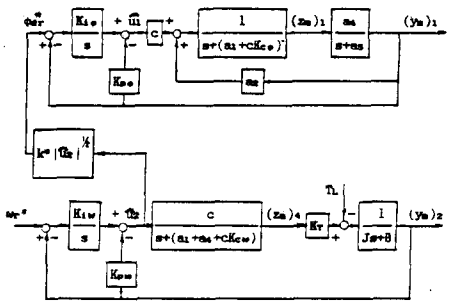

Fig.2.1. The block diagram of the system (2.12)

### 3.Simulations and Experiments

The practical use of our controller developed in the preceding section is examined through simulations and experiments. The tested induction motor is a squirrel cage type with 4 pair poles, rated power 2.2 kW, and rated speed 1750 rpm. The nominal values of its parameters are listed in table 3.1. The controller gains used in the simulations and experiments are

$$K_{p\phi}=104.295 \quad K_{i\phi}=1210.0 \quad K_{c\phi}=3.0$$
$$K_{p\omega}=0.424 \quad K_{i\omega}=1.997 \quad K_{c\omega}=0.522 \qquad (3.1)$$

Before presenting simulation and experimental results, we describe the microprocessor based control system used as a test bed for our controller. As is shown in Fig.3.1, it consists of a 16 bit microprocessor (Motolora 68000) with the CPU clock rate of 8 MHz, a 3 kW peak rated PWM inverter, and the pre-described squirrel cage in-

Table 3.1. Nominal parameters of the tested induction motor.

| 220V/380V, 60Hz, Delta-Connected Stator | | | |
|---|---|---|---|
| $R_s$ | 0.687Ω | $R_r$ | 0.842Ω |
| $L_m$ | 83.97mH | $L_r$ | 85.28mH |
| M | 81.36mH | J | 0.03Kgm² |
| B | 0.01Kgm²/s | $\sigma$ | 0.0756 |
| $i_{ds}$(rated) | 5.9A | $i_{qs}$(rated) | 11A |

duction motor. Signals between the microprocessor and the induction motor are processed through 12bit A/D converters, D/A converters, and 6821 peripheral interface adapters. The rotor speed and position are detected by 6840 counter/timers and an optical encoder whose resolution is 4000 pulses/rev. The DC generator with rated power 2.2 kW and rated speed 1750 rpm was coupled with the induction motor for the load test.

The $2\phi$-$3\phi$ coordinate transformation in Fig.3.1 is required to convert the control inputs for d-q axis stator voltages into those for the actual phase voltages. It is given by

$$\begin{bmatrix} V_{as} \\ V_{bs} \\ V_{cs} \end{bmatrix} = \begin{bmatrix} \sin\theta_s & \cos\theta_s \\ -\sin(\theta_s+\pi/3) & -\sin(\theta_s-\pi/6) \\ -\sin(\theta_s-\pi/3) & -\sin(\theta_s+\pi/6) \end{bmatrix} \begin{bmatrix} V_{ds} \\ V_{qs} \end{bmatrix} \quad (3.2)$$

where $\theta_s = \int \omega_s \, dt$.

On the other hand, the $3\phi$-$2\phi$ coordinate transformation is to convert the measured stator phase currents into the corresponding values in the rotating d-q coordinate system. It is given by

$$\begin{bmatrix} i_{ds} \\ i_{qs} \end{bmatrix} = \begin{bmatrix} \sin(\theta_s-\pi/6) & -\cos\theta_s \\ \sin(\theta_s+\pi/3) & \sin\theta_s \end{bmatrix} \begin{bmatrix} i_{as} \\ i_{bs} \end{bmatrix} \quad (3.3)$$

The overall control algorithm composed of (2.4)-(2.8), (3.2), and (3.3) is executed every 0.5ms on the Motolora 68000 microprocessor.

Two cases are examined in both simulations and experiments. In practice, the optimal slip speed function $f(\omega_r^*)$ is obtained numerically or experimentally. Our interest is not to find $f(\omega_r^*)$ but to show the feasibility of our controller for power efficiency control. Therefore, we assume without loss of generality:

$$k^* = 0.0374 \quad (3.4)$$

In the first case, $\omega_r^*$ is changed from 800 rpm to 1200 rpm at 0.4 sec. Fig.3.2(a) and Fig.3.3(a) show the simulation and experimental responses of the first case. Both the rotor speed and flux responses are satisfactory. Note that $\phi_{dr}$ is automatically adjusted to be 0.364 Wb at steady

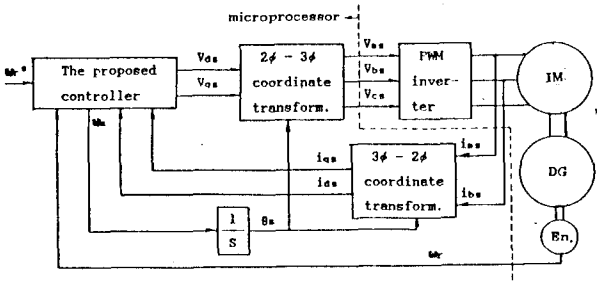


Fig.3.1. Configuration of the control system.

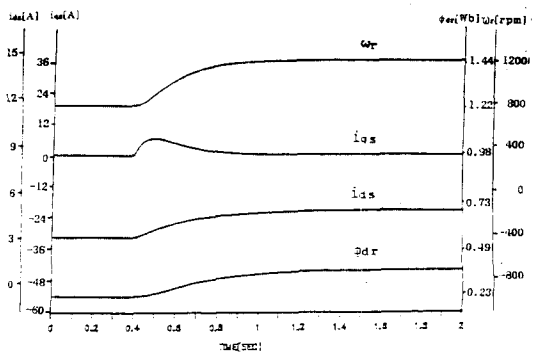


(a) Responses for a step command of $\omega_r^*$.

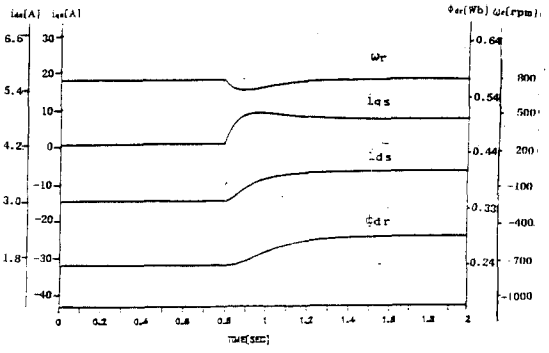


(b) Responses for a step load torque.

Fig.3.2. Simulation results

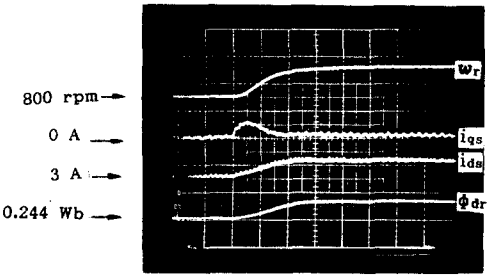


$\omega_r$:400rpm/div. $i_{qs}$:10A/div. $i_{ds}$:3A/div.
$\phi_{dr}$:0.24WB/div. x-axis:0.2sec/div.
(a) Responses for a step command of $\omega_r^*$.

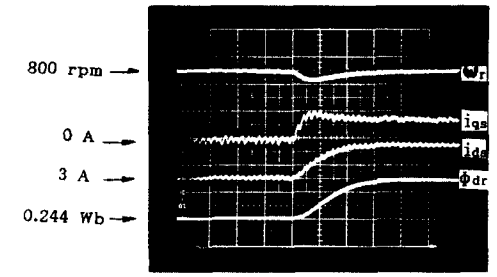


$\omega_r$:200rpm/div. $i_{qs}$:10A/div. $i_{ds}$:0.46A/div.
$\phi_{dr}$:0.03WB/div. x-axis:0.2sec/div.
(b) Responses for a step load torque.

Fig.3.3. Experimental results

state which corresponds to $\omega_{sl}^*$=5.7 rpm at $\omega_r^*$=1200 rpm. In the second case, the half of the rated torque is applied at 0.8 sec, while $\omega_r^*$ is set 800 rpm. Fig.3.2(b) and Fig.3.3(b) show that $\phi_{dr}$ is automatically changed to keep the optimal slip speed determined by (3.4). Thus, the controller given by (2.4)-(2.8) can provide good rotor speed responses as well as high power efficiency.

As can be seen from Fig.3.2-Fig.3.3, the experimental results agree well with the simulation results. However, our experimental results differ slightly from simulation results. That may result from mainly two reasons. First, the control algorithm is performed through 16 bit word operations in the microprocessor, so there exist quantization errors, roundoff errors, and truncation errors. Second, there exist mismatches between the actual parameters of the induction motor and those used in the simulations. Such parameter uncertainties may arise from magnetic saturation, change of temperature, and so on.

## 4.Conclusion

Through simulations and experiments, we have shown that the proposed control method can be effectively used in induction motor control to achieve high power efficiency as well as high dynamic performance. Comparison of the results affirms that the proposed control method is robust against modelling uncertainties. However, aging effect or high temperature may bring in larger modelling uncertainties and, in turn, can degenerate its performance badly. Further researches should be directed toward improving the proposed method in the respects of computational load and robustness against large modelling uncertainties.

## Nomenclature

| | |
|---|---|
| $V_{ds}$ ($V_{qs}$) | d-axis (q-axis) stator voltage |
| $V_a$ ($V_b$, $V_c$) | stator phase voltages |
| $i_{ds}$ ($i_{qs}$) | d-axis (q-axis) stator current |
| $i_a$ ($i_b$, $i_c$) | stator line currents |
| $\phi_{dr}$ ($\phi_{qr}$) | d-axis (q-axis) rotor flux |
| $\omega_r$ | rotor angular speed |
| $\omega_{sl}$ | slip angular speed |
| $\omega_{sl}^*$ | optimal slip angular speed for maximum power efficiency |
| $R_s$ ($R_r$) | stator (rotor) resistance |
| $L_s$ ($L_r$) | stator (rotor) self-inductance |
| $L_M$ | stator/rotor mutual inductance |
| p | the number of pole pairs |
| $\sigma$ | $1-M^2/L_s L_r$ : leakage coefficient |
| c | $1/\sigma L_s$ |
| $a_1$ | $c(R_s+M^2R_r/L_r^2)$ |
| $a_2$ | $cMR_r/L_r^2$ |
| $a_3$ | $cM/L_r$ |
| $a_4$ | $R_r/L_r$ |
| $a_5$ | $MR_r/L_r$ |
| J | rotor inertia of MG set |
| B | damping coefficient of MG set |
| $T_L$ | torque disturbance |
| $\|x\|$ | the Euclidean norm of $x \in R^n$ |
| $\Omega_1 \times \Omega_2$ | a compact subset of $R^2$ |
| $\Omega_x$ | a compact subset of $R^8$ such that $\Omega_x \cap \{x \in R^8 : x_8 = 0\} = \phi$ |
| $\lambda_m(M)$ | the minimum eigenvalue of a symmetric matrix M |

## Appendix A

(1) F, G, and H in (2.9):

$$F(x,\omega_r^*)=\begin{bmatrix} -(a_1+cK_{c\phi})x_1+a_2x_2+cK_{i\phi}x_3-cK_{p\phi}x_8+pa_3x_5x_7 \\ a_5x_1-a_4x_2+a_5\dfrac{x_4x_7}{x_8} \\ \left[\dfrac{ca_5(-K_{c\omega}x_2x_4-K_{p\omega}x_5+K_{i\omega}x_6)}{(a_1+a_4+cK_{c\omega})f(\omega_r^*)}\right]^{1/2}-x_8 \\ -(a_1+cK_{c\omega})x_4+a_2x_7-pa_3x_5(x_2-x_8)-\dfrac{a_5x_1x_4+c(K_{p\omega}x_5-K_{i\omega}x_6)}{x_8} \\ -\dfrac{Bx_5}{J}+\dfrac{K_T(x_2x_4-x_1x_7)}{J} \\ -x_5 \\ a_5x_4-a_4x_7-a_5\dfrac{x_2x_4}{x_8} \\ a_5x_1-a_4x_8 \end{bmatrix},$$

$$G(x)=[0\ 0\ 0\ 0\ 0\ 1\ 0\ 0],\qquad H=\left[0\ 0\ 0\ \frac{1}{J}\ 0\ 0\ 0\right]^T.$$

(2) A, B, f, h, and $\hat{H}$ in (2.11):

$$A=\left[\begin{array}{ccc|ccc} -(a_1+cK_{c\phi}) & a_2-cK_{p\phi} & cK_{i\phi} & 0 & 0 & 0 \\ a_5 & -a_4 & 0 & 0 & 0 & 0 \\ 0 & -1 & 0 & 0 & 0 & 0 \\ \hline 0 & 0 & 0 & -(a_1+a_4+cK_{c\omega}) & -cK_{p\omega} & cK_{i\omega} \\ 0 & 0 & 0 & \dfrac{K_T}{J} & -\dfrac{B}{J} & 0 \\ 0 & 0 & 0 & 0 & -1 & 0 \end{array}\right],$$

$$\hat{H}^T=\left[0\ 0\ 0\ \vdots\ 0\ -\frac{1}{J}\ 0\right],\qquad B^T=\left[\begin{array}{ccc|ccc} 0 & 0 & 1 & 0 & 0 & 0 \\ \hline 0 & 0 & 0 & 0 & 0 & 1 \end{array}\right],$$

$$f(w)=\begin{bmatrix} pa_3z_5 & cK_{p\phi} \\ \dfrac{a_5z_4}{z_2(z_2-e_2)} & 0 \\ 0 & 1 \\ \hline \dfrac{a_5z_4^2}{z_2^2(z_2-e_2)}+a_2z_2 & \dfrac{cz_2(K_{i\omega}z_6-K_{p\omega}z_5)-a_5z_1z_4}{z_2(z_2-e_2)}-pa_3z_2z_5 \\ -\dfrac{K_T}{J}z_1 & 0 \\ 0 & 0 \end{bmatrix},$$

$$g_1(w,\omega_r^*)^T=\left[\begin{array}{cc|ccc} 0 & 0 & g_{23} & 0 & 0 & 0 \\ \hline 0 & 0 & 0 & 0 & 0 & 0 \end{array}\right],\qquad g_2(w,\omega_r^*)^T=\left[\begin{array}{cc|ccc} 0 & 0 & g_3 & 0 & 0 & 0 \end{array}\right],$$

$$g_{23}=\left[\frac{ca_5}{(a_1+a_4+cK_{c\omega})f(\omega_r^*)}\right]^{1/2}\frac{K_{c\omega}z_4}{(\sqrt{K(z)+K_{i\omega}e_2z_4/z_2}+\sqrt{K(z)})z_2},$$

$$K(z)=-K_{c\omega}z_4-K_{p\omega}z_5+K_{i\omega}z_6,\qquad g_3=\left[\frac{ca_5(-K_{c\omega}x_2x_4-K_{p\omega}x_5+K_{i\omega}x_6)}{(a_1+a_4+cK_{c\omega})f(\omega_r^*)}\right]^{1/2},$$

$$h(w)=\begin{bmatrix} -a_4 & \dfrac{-a_5z_4}{z_2(z_2-e_2)} \\ \dfrac{a_5z_4}{z_2(z_2-e_2)} & -a_4 \end{bmatrix}.$$

## Reference


[1] F. Blaschke, "The Principle of Field Orientation as Applied to the New TRANSVECTOR Closed-Loop Control System for Rotating Field Machines," Simens Review, vol.34, pp.217-220, 1972.

[2] R. D. Lorenz and D. B. Lawson, "Performance of Feedforward Current Regulators for Field-Oriented Induction Machine Controllers," I.E.E.E. Trans. Ind. Appl., vol.23, no.4, pp.597-602, 1987.

[3] F. Harashima, S. Kondo, K. Ohnishi, M. Kajita, and M Susono, "Multimicroprocessor-Based Control System For Quick Response Induction Motor Drive," I.E.E.E. Trans. Ind. Appl., vol.21, no.4, pp.602-609, 1985.

[4] Y. Kuroe and H. Haneda, "Theory of Power-Electronics AC Motor Control for Modeling, Estimation, and Control and/or Analysis," Proceeding of the 26th CDC, pp.54-61, 1986.

[5] K. Ohnishi, H. Suzuki, K. Miyachi, and M. Terashima, "Decoupling Control of Secondary Flux and Secondary Current in Induction Motor Drives with Rotor Time Constant Identification Function," I.E.E.E Trans. Ind. Appl., vol.21, no.1, pp.241-246, 1986.

[6] W. Leohnard, "Microprocessor Control of High Dynamic Performance ac-Drives-A Survey," Automatica, vol.22, no.1, pp.1-19, 1986,

[7] A. Kusko and D. Galler, "Control Means for Minimization of losses in AC and DC Motor Drives," I.E.E.E Trans. Ind. Appl., vol.19 ,No.4, pp.561-570, 1983.

[8] M .H. Park and S. K. Sul, "Microprocessor-Based Optimal-Efficiency Drive of an Induction Motor," I.E.E.E. Trans. Ind. Elec., vol.31, no.1, pp.69-73, 1984.

[9] H. G. Kim, S. K. Sul, and M. H. Park, "Optimal Efficiency Drive of a Current Source Inverter Fed Induction Motor by Flux Control," I.E.E.E Trans. Ind. Appl., vol.20 ,No.6, pp.1453-1459, 1984.

[10] D. S. Kirschen, D. W. Novotny, and T. A. Lipo, "Optimal Efficiency of an Induction Motor Drive," I.E.E.E Trans. Energy Conver., vol.2 , no.1, pp.70-75, 1987.

[11] M. Murata, T. Tsuchiya, and I. Takeda, "A New Synthesis Method for Efficiency Optimized Speed Control System of Vector-Controlled Induction Machine," PESC'88, vol.2, pp862-869

[12] B. Jakubczyk and W. Respondeck, "On Linearization of Control Systems," Bull. Acad. Pol. Sci. Math., vol.28, pp.517-520, 1980.

[13] A. Isidori, A. J. Krener, and C. Gori-Giorgi, and S. Monaco, "Nonlinear Decoupling via Feedback: A Differential Geometric Approach," I.E.E.E Trans. Automat. Contr., vol.26, pp.331-345, 1981.

[14] L. R. Hunt, R. Su, and G. Meyer, "Global Linearization of Nonlinear Systems," I.E.E.E Trans. Automat. Contr., vol.28, pp.24-31, 1983.

[15] H. Nijmeijer, "Feedback Decomposition of Nonlinear Control Systems," IEEE Trans. Automat. Contr., vol.28, pp.861-862, 1983.

[16] I. J. Ha, "The Standard Decomposed System and Noninteracing Feedback Control of Nonlinear Systems," SIAM J. Contr. and Optim., vol.26, no.5, pp.1-14, 1988.

[17] Z. Krzeminski, "Nonlinear Control of Induction Motor," 10th IFAC Conference, vol.3, pp.349-354, 1987.

[18] A. D. Luca and Giovanni U., "Full Linearization of Induction Motors via Nonlinear State-Feedback," Proceeding of the 26th CDC, pp.1765-1770, 1987.

[19] D. I. Kim, M. S. Ko, I. J. Ha, and J. W. Park, "Asymptotic Decoupled Control of Rotor Speed and Flux in Induction Motors," SICE'88, vol.2, pp.847-851.

[20] A. B. Plunkett, "Direct Flux and Torque Regulation in PWM Inverter-Induction Motor Drive," I.E.E.E. Trans. Ind. Appl., vol.13, no.2, pp.139-146, 1977.

[21] M. Koyama, M. Yano, I. Kamiyama, and S. Yano, "Microprocessor-Based Vector Control System for Induction Motor Drives with Rotor Time Constant Identification Function," I.E.E.E Trans. Ind. Appl., vol.21, no.3, pp.453-459, 1986.

[22] L. J. Garces, "Parameter Adaption for the Speed-Controlled Static AC Drive with a Squirrel-Cage Induction Motor," I.E.E.E. Trans. Ind. Appl., vol.16, no.2, pp.173-178, 1980.

[23] Y. Hori, V. Cotter, and Y. Kaya, "A Novel Induction Motor Flux Observer and Its Application to a High Performance AC drive Systems," 10th IFAC Conference, vol.3, pp.355-pp.360, 1987.

[24] G. C. Verghese and S. R. Sanders, "Observers for Flux Estimation in Induction Motors," IEEE Trans.Ind. Elec., vol.35, no.1, pp.85-94, 1988

[25] P. K. Nandam and P. C. Sen, "A Comparative Study of Proportional-integral(P-I) and Integral-proportional(I-P) Controllers for DC Motor Drives," Int. J. Control, vol.44, no.1, pp.283-297, 1986.